Japanese URSI Commission H (Waves in Plasmas)
Activity Report
March 2014 - June 2014

[1] Status of projects related with plasma wave observation

- NICT Science Cloud

  NICT Science Cloud has been developed for space plasma studies. We have begun to develop a Web application for plasma wave data and other satellite observation data, which is named “STARStouch”. This Web application is based on a technique of asynchronous data transfer of graphic files for several types of data plots. The cloud system create a huge number of data plots with various time scale (e.g., from few minutes to few years) for each data-set. Users can preview time-dependent observation data of such multi-time scale plots with easy operations (tap, pinch, drag, flick…). Plasma wave (Figure 1), plasma particle, magnetic fields and orbit data of the GEOTAIL satellite are available on the STARStouch GEOTAIL. We have opened this Web site in May 2014.

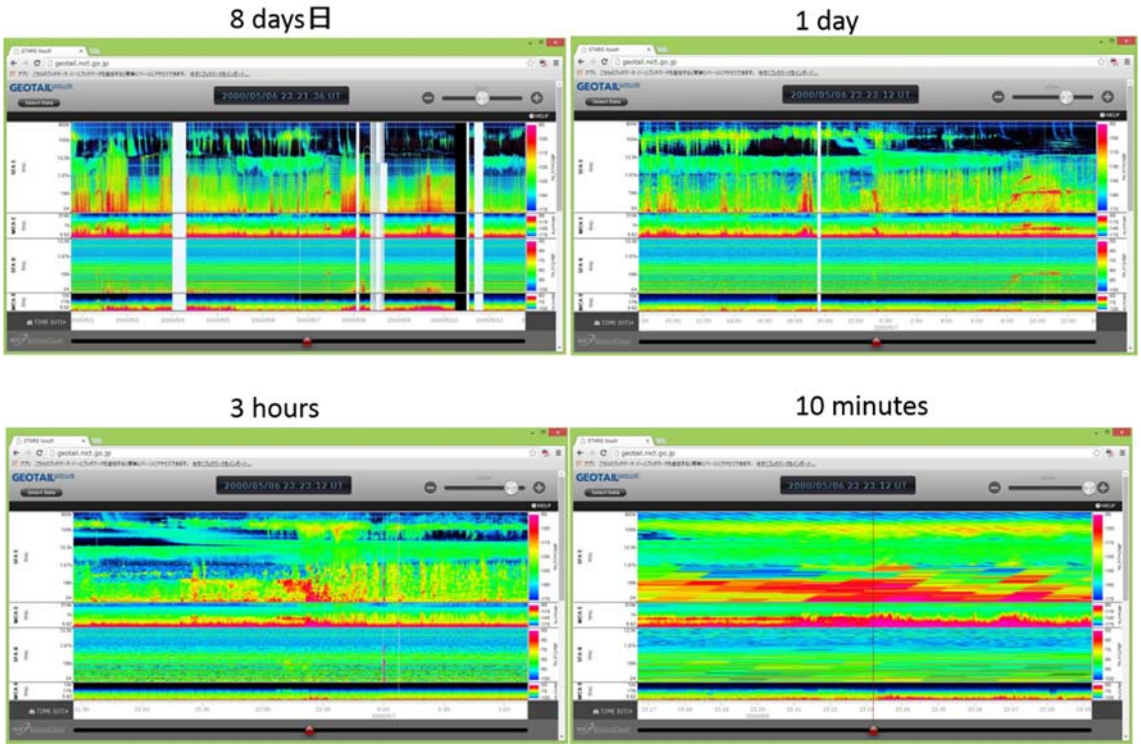

Figure 1: STARStouch GEOTAIL version: http://geotail.nict.go.jp

[2] Recent Meetings

1. Japan Geoscience Union Meeting 2014, Yokohama, Japan, 28 April – 2 May, 2014.
2. ISRSSP 2014 (Fourth International Symposium on Radio Systems and Space Plasma) , Luxembourg, 26-27, June, 2014.
3. AOGS 2014, Sapporo, Japan, 28 July – 1 August, 2014.

[3] Future Meetings

1. The 40th COSPAR Scientific Assembly, Moscow, Russia, 2-10 August, 2014.
2. The 31st URSI GASS, Beijin, China, 16-23 August, 2014.
3. AGU Chapman Conference on "Low Frequency Waves in Space Plasmas", Jeju, Korea, 31 August - 5 September, 2014.
4. Geospace revisited: a Cluster / MAARBLE / Van Allen Probes Conference, Rhodes, Greece, 15-20 September, 2014
5. The 12th International Conference on Substorms, Ise, Japan, 10-14 November, 2014.

[4] Recently Published Papers (March 2014 – June 2014)

1. **Toshihiro Habagishi, Satoshi Yagitani, and Yoshiharu Omura, Nonlinear damping of chorus emissions at local half cyclotron frequencies observed by Geotail at L > 9, J. Geophys. Res. Space Physics, Vol.119, pp.4475-4483, doi:10.1002/2013JA019696, May 2014.**

   A statistical analysis of upper band and lower band chorus emissions observed by the Geotail spacecraft has been performed. Chorus elements are generated near the magnetic equator (or the high-latitude minimum-B pockets in the outer magnetosphere) as discrete emissions covering a frequency range of 0.1-0.65 fce0, where fce0 is the cyclotron frequency in the generation region, with wave vectors parallel to the ambient magnetic field. As the emissions propagate away from the generation region, it is possible that they undergo the nonlinear damping at half the local cyclotron frequency 0.5 fce because of the quasi-parallel propagation. The nonlinear damping can separate the emissions into the upper band and lower band chorus emissions. It has been found that the lower cutoff of the upper band emissions coincides with 0.5 fce, while the upper cutoff of the lower band emissions represents 0.5 fce0. When 0.5 fce exceeds 0.65 fce0, the chorus emission is observed as a lower band-only emission.

2. **Satoshi Yagitani, Toshihiro Habagishi, and Yoshiharu Omura, Geotail observation of upper-band and lower-band chorus elements in the outer magnetosphere, J. Geophys. Res. Space Physics, Vol.119, pp.4694-4705, doi:10.1002/2013JA019678, June 2014.**

Using the Geotail observation of upper band and lower band (dual-band) rising tone chorus waveforms in the dayside outer magnetosphere (L~10.5), it has been found that the lower cutoff frequency of the upper band elements follows half the local gyrofrequency, whereas the upper cutoff of the lower band elements is almost consistent with half the gyrofrequency at a minimum-B pocket (a possible chorus generation region) according to the Tsyganenko geomagnetic model. This is consistent with the scenario that the rising tone wave packet initially excited in a wide frequency range suffers from damping at half the local gyrofrequencies during quasi-parallel propagation. Since the local gyrofrequency gradually increases away from the generation region, the upper cutoff of a lower band element should represent half the gyrofrequency at the generation region, whereas the lower cutoff of an upper band element should follow half the local gyrofrequency. It has been confirmed that the frequency sweep rates and amplitudes of the observed chorus wave packets are consistent with those predicted by the nonlinear growth theory of chorus emissions, except for the frequency gap.

3. **S. Matsuda, Y. Kasahara, and Y. Goto, High-altitude M/Q=2 ion cyclotron whistlers in the inner magnetosphere observed by the Akebono Satellite, Geophys. Res. Lett., 41, 3759–3765, doi:10.1002/2014GL060459, 2014.**

   An ion cyclotron whistler is a left-handed polarized electromagnetic ion cyclotron mode wave converted from a lightning electron whistler. In the paper, M/Q = 2 ion cyclotron whistlers observed by Akebono in the altitude region around 3200–10000 km (L = 1.5–3.4) was introduced. The observation point was a considerably higher altitude than those previously reported, which indicates that M/Q = 2 ions are present not only in the low-altitude region but also in the inner magnetosphere around L = 3.4. They also demonstrated that the concentration of M/Q = 2 ions around 4200 km (L = 1.7) during this event was plausibly up to 12.6%. This result gives important clues to study unknown minor ion profiles such as circulation mechanism of deuterons or injection mechanism of alpha particles in the solar wind.

4. **S. Matsuda, Y. Kasahara, and Y. Goto, Electromagnetic ion cyclotron waves suggesting minor ion existence in the inner magnetosphere observed by the Akebono satellite, J. Geophys. Res. Space Physics, 119, 4348–4357, doi:10.1002/2013JA019370, 2014.**

   EMIC waves in the vicinity of the geomagnetic equator exhibiting a sudden decrease in intensity (characteristic lower cutoff) at just above half of the proton cyclotron frequency were reported. The waves were observed by Akebono along its trajectory during a magnetic storm in April 1989. They demonstrated that the waves propagate with a large wave normal angle with respect to the geomagnetic field line and that they had a crossover frequency above the characteristic lower

cutoff. The characteristic frequencies of each event did not vary despite disturbances in the inner magnetosphere, represented by a sudden decrease in the Dst index and electron density fluctuation. In addition, the waves were repeatedly observed within a half day after sudden decreases in Dst; however, they disappeared when the recovery of the Dst index became moderate. Matsuda et al. suggested that wave generation appears to be closely correlated to fresh energetic particle injection, and that the existence of a few percent of alpha particles (He++) or deuterons (D+) can explain the lower cutoff of the EMIC waves under the condition of multiple ion species.

5. **O. V. Agapitov, A. V. Artemyev, D. Mourenas, Y. Kasahara, and V. Krasnoselskikh, Inner belt and slot region electron lifetimes and energization rates based on AKEBONO statistics of whistler waves, J. Geophys. Res. Space Physics, 119, 2876–2893, doi:10.1002/2014JA019886, 2014.**

   Global statistics of the amplitude distributions of hiss, lightning-generated, and other whistler mode waves from terrestrial VLF transmitters have been obtained from Akebono in the Earth's plasmasphere and fitted as functions of L and latitude for two geomagnetic activity ranges (Kp<3 and Kp>3). In particular, the present study focuses on the inner zone L∈[1.4,2] where reliable in situ measurements were lacking. Based on this statistics, simplified models of each wave type are presented, and quasi-linear pitch angle and energy diffusion rates of electrons by the full wave model are calculated. Corresponding electron lifetimes compare well with decay rates of trapped energetic electrons obtained from Solar Anomalous and Magnetospheric Particle Explorer and other satellites at L∈[1.4,2].

6. **Murata, K., Watanabe, H., Ukawa, K., Muranaga, K., Suzuki, Y., Isoda, F., Yamamoto, K., Kubota, Y., Nagatsuma, T., Sakaguchi, K., Tsugawa, T., Nishioka, M., Tatebe, O., Tanaka, M., Fukazawa, K., Saita, S., Ebihara Y., Fujita, S., Kimura, E., Kurosawa, T., Murayama, Y., Nagai, T., and Mizuhara T. The NICT Science Cloud-A Proposal of Cloud System for Scienti.c Researches-, Journal of Space Science Informatics Japan(ISSN 1349-1113), Vol.3(2014), pp.39-56, 2014.**

   This paper is to propose a cloud system for science, which has been developed at NICT (National Institute of Information and Communications Technology), Japan. The NICT science cloud is an open cloud system for scientists who are going to carry out their informatics studies for their own science. The NICT science cloud is not for simple uses. Many functions are expected to the science cloud; such as data standardization, data collection and crawling, large and distributed data storage system, security and reliability, database and meta-database, data stewardship, long-term data preservation, data rescue and preservation, data mining, parallel processing, data publication and provision, semantic web, 3D and 4D visualization, out-reach and in-reach, and

capacity buildings.

7. **Murata, K., ISODA, F., Watanabe, H., Fukazawa, K., Yamamoto, K., Tatebe, O., Tanaka, M., and Kimura, E. High Performance Visualization Processing of Large-Scale Computer Simulation Data via NICT Science Cloud, Journal of Space Science Informatics Japan(ISSN 1349-1113), Vol.3(2014), pp.57-70, 2014.**

   Science cloud is a cloud system designed for scienti.c researches, and expected as a new infrastructure for big data sciences. Not only parallelization of CPU as in super-computers, but I/O and network throughput parallelization are crucial for the big data sciences. One of the typical structures of science cloud is a scalable cluster in which multiple clusters in a cloud are connected with high-speed network. In the present study, we examine performance of parallelization of both CPU and I/O in a cloud system as the .rst step to high performance scalable clusters. In case with few processes executed on each computational node (server), parallelization ef.ciency is almost 100%. This high ef.ciency is expected to maintain in larger-scale cluster systems such as those with 100 servers. On the condition of multi-processes on each node, the present parallelization does not show good performance due to the congestions of I/O. Parallelization ef.ciency (speed-up) is as low as 20.6%. New techniques of decentralization of I/O within each node are required in the next step.

8. **Kubota, Y., Murata, K. T., Yamamoto, K., Fukazawa, K. and Tsubouchi, K., Visualization technique using a system of Magnetic Field Tracing in Global MHD simulations, Journal of Space Science Informatics Japan(ISSN 1349-1113), Vol.3(2014), pp.129-135, 2014.**

   We developed a system of Magnetic Field Tracing in Global MHD simulations in order to understand magnetosphere convection. To trace magnetic flux tube with high precision, we need to process big data such as all time-series simulation data. In this paper, we show a parallel distribution visualization technique for magnetic field tracing by using NICT science cloud.

9. **Murata, K. T., Watanabe, H., Yamamoto, K., Kimura, E., Tanaka, M., Tatebe, O., Ukawa, K., Muranaga, K., Suzuki, Y. and Kojima, H., A high-speed data processing technique for time-sequential satellite observation data, IEICE Communications Express, Vol.3(2014), No.2, pp.74-79, 2014..**

   A variety of satellite missions are carried out every year. Most of the satellites yield big data, and high-performance data processing technologies are expected. We have been developing a cloud system (the NICT Science Cloud) for big data analyses of Earth and Space observations via spacecraft. In the present study, we propose a new technique to process big data considering the fact that high-speed I/O (data file read and write) is important compared with data processing

speed. We adopt a task scheduler, the Pwrake, for easy development and management of parallel data processing. Using a set of long-time scientific satellite observation data (GEOTAIL satellite), we examine the performance of the system on the NICT Science Cloud. We successfully archived high-speed data processing more than 100 times faster than those on traditional data processing environments.

10. **Shoji, M., and Y. Omura, Spectrum characteristics of electromagnetic ion cyclotron triggered emissions and associated energetic proton dynamics, J. Geophys. Res. Space Physics, 119, doi:10.1002/2013JA019695, 2014.**

    We perform parametric analyses of electromagnetic ion cyclotron (EMIC) triggered emissions with a gradient of the nonuniform ambient magnetic field using a hybrid simulation. According to nonlinear wave growth theory, as the gradient of the ambient magnetic field becomes larger, the theoretical threshold of the wave amplitude becomes larger, although the optimum wave amplitude for nonlinear wave growth does not change. With a larger magnetic field gradient, we obtain coherent rising-tone spectra because the triggering process of the EMIC triggered emission takes place only under a limited condition on the wave amplitude. On the other hand, with a smaller magnetic field gradient, triggering of the emissions can be caused with various wave amplitudes, and then the subpackets are generated at various locations at the same time. The concurrent triggering of emissions results in incoherent waves, observed as “broadband” EMIC bursts.

11. **Nakamura, S., Y. Omura, S. Machida, M. Shoji, M. Nosé, and V. Angelopoulos, Electromagnetic ion cyclotron rising tone emissions observed by THEMIS probes outside the plasmapause, J. Geophys. Res. Space Physics, 119, 1874–1886, doi:10.1002/2013JA019146, 2014.**

    We report observations of electromagnetic ion cyclotron (EMIC) triggered emissions observed by the Time History of Events and Macroscale Interactions during Substorms (THEMIS) probes outside the plasmasphere. Although these phenomena have recently received much attention because of the possibility of strong interaction with particles, only a few events of EMIC triggered emissions have been reported near the equatorial plasmapause. We performed a survey of the THEMIS probe data and found various types of emissions mainly on the dayside at radial distances of 6–10 RE. We study three distinctive events in detail. The first is a typical event with an obvious rising tone emission in the afternoon sector. The emissions in the second event are simultaneously excited in different frequency bands separated by the cyclotron frequency of helium ions. In the third event, which occurred near local noon, rising tone emissions were excited in an extended region near the equator where the field-aligned B gradient was much

reduced because of compression of the magnetosphere by the solar wind. We compare these events with the nonlinear wave growth theory developed by Omura et al. (2010). In all events, it is found that the observed relationship between the amplitudes and frequencies of the emissions are in good agreement with the theory.

12. **Y. Katoh, K. Iwai, Y. Nishimura, A. Kumamoto, H. Misawa, F. Tsuchiya, and T. Ono, Generation mechanism of the slowly drifting narrowband structure in the Type IV solar radio bursts observed by AMATERAS, Astrophys. J., 787,45, doi:10.1088/0004-637X/787/1/45, 2014.**

We investigate the type IV burst event observed by AMATERAS on 2011 June 7, and reveal that the main component of the burst was emitted from the plasmoid eruption identified in the EUV images of the Solar Dynamics Observatory (SDO)/AIA. We show that a slowly drifting narrowband structure (SDNS) appeared in the burst's spectra. Using statistical analysis, we reveal that the SDNS appeared for a duration of tens to hundreds of milliseconds and had a typical bandwidth of 3MHz. To explain the mechanism generating the SDNS, we propose wave-wave coupling between Langmuir waves and whistler-mode chorus emissions generated in a post-flare loop, which were inferred from the similarities in the plasma environments of a post-flare loop and the equatorial region of Earth's inner magnetosphere. We assume that a chorus element with a rising tone is generated at the top of a post-flare loop. Using the magnetic field and plasma density models, we quantitatively estimate the expected duration of radio emissions generated from coupling between Langmuir waves and chorus emissions during their propagation in the post-flare loop, and we find that the observed duration and bandwidth properties of the SDNS are consistently explained by the proposed generation mechanism. While observations in the terrestrial magnetosphere show that the chorus emissions are a group of large-amplitude wave elements generated naturally and intermittently, the mechanism proposed in the present study can explain both the intermittency and the frequency drift in the observed spectra.

13. **Teramoto, M., N. Nishitani, V. Pilipenko, T. Ogawa, K. Shiokawa, T. Nagatsuma, A. Yoshikawa, D. Baishev, and K. T. Murata, Pi2 pulsation simultaneously observed in the E and F region ionosphere with the SuperDARN Hokkaido radar, J. Geophys. Res., doi: 10.1002/2012JA018585, 2014**

We investigated Pi2 pulsations in the nightside ionosphere that began at 14:15 UT (2315 LT) on 11 July 2010, and they were observed with high-temporal (8 s) resolution by beam 4 of the Super Dual Auroral Radar Network (SuperDARN) Hokkaido radar. These pulsations were simultaneously observed in both the ground/sea scatter echoes reflected from the *F* region height and in ionospheric echoes from field-aligned irregularities in the sporadic E_s region.

They had the same period of 110 s and approximately no phase lag. From the radar observations and the International Geomagnetic Reference Field model, the amplitude of the eastward (E_{EW}) component of the electric field of the Pi2 pulsations in the ionosphere was estimated ~8.0 mV/m in the *F* region and ~2.0 mV/m in the *E* region. Corresponding Pi2 pulsations appeared dominantly in the horizontal northward magnetic field component (*H*) at nearby ground stations, Moshiri (MSR), St. Paratunka (PTK), and Stecolny (STC), with amplitudes ranging from 6 nT (MSR) to 10 nT (STC). At the dominant frequency of 8.8 mHz, the coherences between *H* and E_{EW} were high (>0.9), the cross phases of E_{EW} relative to *H* were −56° and −45°, and the amplitude ratios were 2.7×10^5 m/s and 8.4×10^5 m/s, in the *E* and *F* regions, respectively. Based on a comparison of these results with theoretical predictions, we suggest that the concept of a pure cavity mode is not sufficient to explain the combined observations for midlatitude Pi2 waves and that the contribution of an Alfvén waves must be taken in account.